International
Multidisciplinary
Research Journal
Reviews (IMRJR)

# Cycle-Crafted Superlattices: Exploring SILAR-Induced Enhancements in CdSe/CuSe Thin Films for Solar Applications

**\*Elekalachi, C. I.[1*], Ezenwa, I. A.[1], Okereke, A. N.[1], Okoli, N. L.[2], Nwori, A. N.[1] and Onoh, E. U.[3]**

Department of Industrial Physics, Faculty of Physical Science, Chukwuemeka Odumegwu Ojukwu University Uli, Anambra State, Nigeria[1]

Department of Computer Education, Faculty of Education and Art, Madonna University Nigeria (Okija Campus), Anambra State, Nigeria[2]

Nanoresearch Laboratory, University of Nigeria Nsukka, Enugu State, Nigeria[3]

[*]Corresponding Author's E-mail: ci.elekalachi@coou.edu.ng

**Abstract:** Semiconductor superlattice thin films of CdSe/CuSe were successfully deposited on microscopic glass substrates using SILAR deposition technique. Three SILAR cycles were optimized and the films were subjected for SEM, EDX, UV-Vis and XRD analysis prior to annealing at 423 K for 60 minutes to determine their properties for photovoltaic applications. The SEM image of the CdSe/CuSe superlattice thin film shows the surface contained agglomerated mass of interconnected spherical-like nanoparticles of different sizes. The result of the EDX analysis indicated that more of the Cu-Se atoms are deposited compared to Cd-Se atoms. The optical properties of the films showed that the absorbance and extinction coefficient of the films increased with increase in the SILAR cycles. The film deposited after 10 cycles has the highest absorbance value in the range of 0.75–0.45 in the VIS region and 0.45-0.50 in the NIR, while the film deposited at 2 cycles has lowest value of 0.20–0.10 in the VIS and 0.10 in the NIR region. The bandgap energy was found to decrease as the number of SILAR cycles increased and values obtained are 2.00 eV, 1.95 eV and 1.90 eV for the films deposited at 2, 6 and 10 cycles respectively. These bandgap values are in the range suitable for thin film solar cell and many other optoelectronic applications. Structural analysis revealed that films subjected to a higher number of SILAR cycles exhibited enhanced crystallinity. As the number of SILAR cycles increased, the average crystallite size of the CdSe/CuSe films grew larger. Simultaneously, the dislocation density and micro-strain within the films decreased progressively with the increase in the number of cycles from 6 to 10.

**Keywords**: cadmium selenide, copper selenide, SILAR, bandgap, superlattice, optoelectronics, solar cells

## 1. INTRODUCTION

The stepping up of research in electrical energy generation using thin film photovoltaic systems and solar energy technology have continued to serve as the major contributors of the ongoing energy transition. Though about 1.7% of world electricity is provided by solar cells system considering that entire adsorbed solar energy by the earth is approximately $1 \times 10^{22}$ J per day [1]. Studies have shown that thin film solar energy system has a very great bound for clean and green energy and can serve as a source of energy supply with the capacity to face the long-term energy demands in the world [2, 3]. The properties and efficiency of solar photovoltaic cells are established around the photoelectric effect happening on the semiconductor materials used. In this regard, when the semiconductor material absorbs a photon; there is an electron gain of the energy linked to that photon. These semiconductor materials have nanocrystalline structures and thus possess an unusal size-dependent and electrical characteristic which is described by valence and conduction electrons only in selected values of energy regardless of a forbidden band energies called energy gap that is bridging the valence and conduction electrons [4].

Transition metal chalcogenides based thin films devices have contributed much because of their technological significance in several applications in photoelectric, photocatalysis, and energy harvesting and storage devices [5, 6]. Cadmium selenides (CdSe) and copper selenides (CuSe) are important examples of these metal selenides. CdSe is a II-VI semiconductor with n-type conductivity while CuSe is a I-VI semiconductor compound with p-type conductivity due to copper vacancies which has both direct and indirect bandgap; a property which is useful in the solar cell production [7, 8]. Synthesis of CdSe thin films has been achieved using various deposition methods such as thermal evaporation [9-11], sputtering [12, 13], electron beam evaporation [14,15], molecular beam epitaxy [16], pulsed laser deposition [17], spray pyrolysis [18, 19], sol gel spin coating [20], chemical bath deposition [21-24], electrochemical deposition [25, 26]

and spin-coating method [27]. On the other hand, CuSe thin films have also been synthesized using various deposition techniques such as chemical bath deposition [28-30], thermal evaporation technique [31], electrodeposition method [32-36], spin coating, spray pyrolysis and successive ionic layer adsorption and reaction (SILAR) methods [37].

Furthermore, researches have been focusing recently on different techniques for improving the properties of these metal selenides by synthesizing them in superlattice form which have promising properties that make them good materials for solar cell device application. Semiconductors Superlattice are structures consisting of alternating layers of two different semiconductors materials, for example AlAs/GaAs, ZnS/CdS, $GaAs/GaAs_{1-x}P_x$, Ge/GaAs, and ZnO/MgO etc. It is a structure where two different materials are grown to a specific thickness in alternating layers [38]. The two different materials possess different bandgaps, which leads to discontinuities in both the conduction and valence band [39]. Hamilton *et al* have synthesized thin film CdSe/CuSe photovoltaic on a flexible single walled carbon nanotube substrate [40]. Xu *et al* studied the surface modification and enhancement of luminescence due to quantum effects in coated CdSe/CuSe semiconductor nanocrystals [41]. Kalyanikutty *et al* has also fabricated and studied the ultra-thin crystalline films of CdSe and CuSe that was formed at an organic-aqueous interface [42].

In this research, we fabricated the superlattice thin film structures of CdSe/CuSe using successive ion layer adsorption reaction (SILAR) method to study their properties. This method is preferred because it is inexpensive and convenient for large surface area deposition.

### 2.1 Materials and Method

The materials used in the preparation of the superlattice thin films of CdSe/CuSe in this work include: Cadmium chloride ($CdCl_2$), Copper (II) acetate ($Cu(CH_3COO)_2$), Selenium (IV) oxide ($SeO_2$), Sodium borohydride ($NaBH_4$), Acetone [$(CH_3)_2CO$] and Trioxonitrate (V) acid ($HNO_3$) supplied from Sigma-Aldrich. Other materials used are microscopic glasses and distilled water which were used as substrates and reaction medium respectively. The method employed in the deposition of the superlattice thin films is successive ionic layer adsorption reaction (SILAR) method.

### 2.2 Experimental Procedure

The microscopic glasses used as substrates were initially soaked in concentrated solution of trioxonitrate (V) acid for two days and afterwards washed with detergent-water solution before being rinsed with distilled water. The substrates were subsequently ultra-sonicated in solution of acetone in water of volume ratio (3:1) for 30 minutes at 50℃. Finally, the degreased substrates were rinsed 3 times with distilled water and dried in an electric oven at 60℃ for 30 minutes. The reacting masses of the preferred molar solutions for the pecursors of $Cd^{2+}$, $Cu^{2+}$ and $Se^{2-}$ sources were prepared by dissolving the approptiate masses of the compounds in distilled water using the relation as given by [43].

$$Reacting\ mass = \frac{Molarity \times molar\ mass \times volume}{1000} \qquad\qquad 1$$

For the formation of the CdSe/CuSe superlattice thin films, CdSe films were first prepared on the glass substrate using four beakers in which the first beaker labeled A containing cationic precursors ($CdCl_2$) the second beaker labeled B containing ionic exchange medium (distilled water), beaker C containing anionic precursor (NaHSe) and the beaker labeled D contains ionic exchange medium (distilled water).

The complete SILAR cycle involved the following steps;

Immersion of the cleaned glass substrates in the beaker (A) containing $Cd^{2+}$ precursor solution for 40 s to absorb $Cd^{2+}$ on the surface of the substrate.

The substrates were rinsed distilled water for 10 s to remove excess $Cd^{2+}$ that are loosely adherent to the glass substrates (from the previous step).

The substrates were then immersed in the anionic precursor solution of freshly prepared NaHSe for another 40 s. The selenide ($Se^{2-}$) ions reacted with the absorbed $Cd^{2+}$ on the active center of the substrates to form metal selenide films (CdSe).

Again, the substrates were rinsed in distilled water for 10 s to remove loosely bound ions present on the substrates and unreacted cations and anions and this completed one cycle. These steps were repeated one more time and three samples of CdSe thin films were deposited at different SILAR cycles of 2, 6 and 10 on the glass substrates.

The quantities of the precursors used for the deposition of CdSe thin films are displayed in Table 1

Table 1: Optimization of number of SILAR cycles for cadmium selenide thin films

| Bath Name | Beaker A | Beaker B | Beaker C | Beaker D | Number of SILAR Cycle |
| --- | --- | --- | --- | --- | --- |
| | 0.2 M ($Cd^{2+}$) | $H_2O$ | NaHSe | $H_2O$ | |
| | Vol (ml) | Vol (ml) | Vol (ml) | Vol (ml) | |
| CdSe2 | 80 | 80 | 80 | 80 | 2 |
| CdSe6 | 80 | 80 | 80 | 80 | 6 |
| CdSe10 | 80 | 80 | 80 | 80 | 10 |

The three deposited thin films of CdSe on the glass substrates were thereafter used as potential substrates for deposition of the CdSe/CuSe superlattice thin films. The steps taken above for the deposition of the films of CdSe were followed with the cationic precursor $Cd^{2+}$ in beaker A replaced with solution of $Cu^{2+}$ ion source. The three thin films of CdSe/CuSe were deposited after 2, 6 and 10 cycles and were annealed at temperature of 423 K for 60 minutes. The optimized parameters for the deposited films are shown in Table 2.

Table 2: Optimization of number of SILAR cycles for CdSe/CuSe Superlattice thin films

| Bath Name | Beaker A | Beaker B | Beaker C | Beaker D | Number of SILAR Cycle | Annealing temp. (K) |
| --- | --- | --- | --- | --- | --- | --- |
| | 0.2 M ($Cu^{2+}$) | $H_2O$ | NaHSe | $H_2O$ | | |
| | Vol (ml) | Vol (ml) | Vol (ml) | Vol (ml) | | |
| CdSe/CuSe2 | 80 | 80 | 80 | 80 | 2 | 423 |
| CdSe/CuSe6 | 80 | 80 | 80 | 80 | 6 | 423 |
| CdSe/CuSe10 | 80 | 80 | 80 | 80 | 10 | 423 |

### 2.3  Material Characterizations

The deposited thin films were subjected for morphological, compositional, optical and structural characterizations using scanning electron microscopy (SEM), energy dispersive spectroscopy (EDX), and UV-VIS spectroscopy and x–ray diffraction method to determine their morphological, compositional optical and structural properties. The thickness values of the deposited thin films were characterized using gravimetric method

## 3.  RESULTS AND DISCUSSIONS

### 3.1  Morphological properties the deposited thin films

The SEM micrograph of superlattice thin films of CdSe/CuSe deposited at the different number of SILAR cycles of 2, 6 and 10 is displayed in figure 1. From the figure, it is observed that the surface of the CdSe/CuSe superlattice thin films contained agglomerated mass of interconnected spherical-like nanoparticles of different sizes. Different particle sizes of 44.78 nm, 36.12 nm and 47.65 nm were obtained for films deposited at 2, 6 and 10 SILAR cycle respectively.

International
Multidisciplinary
Research Journal
Reviews (IMRJR)
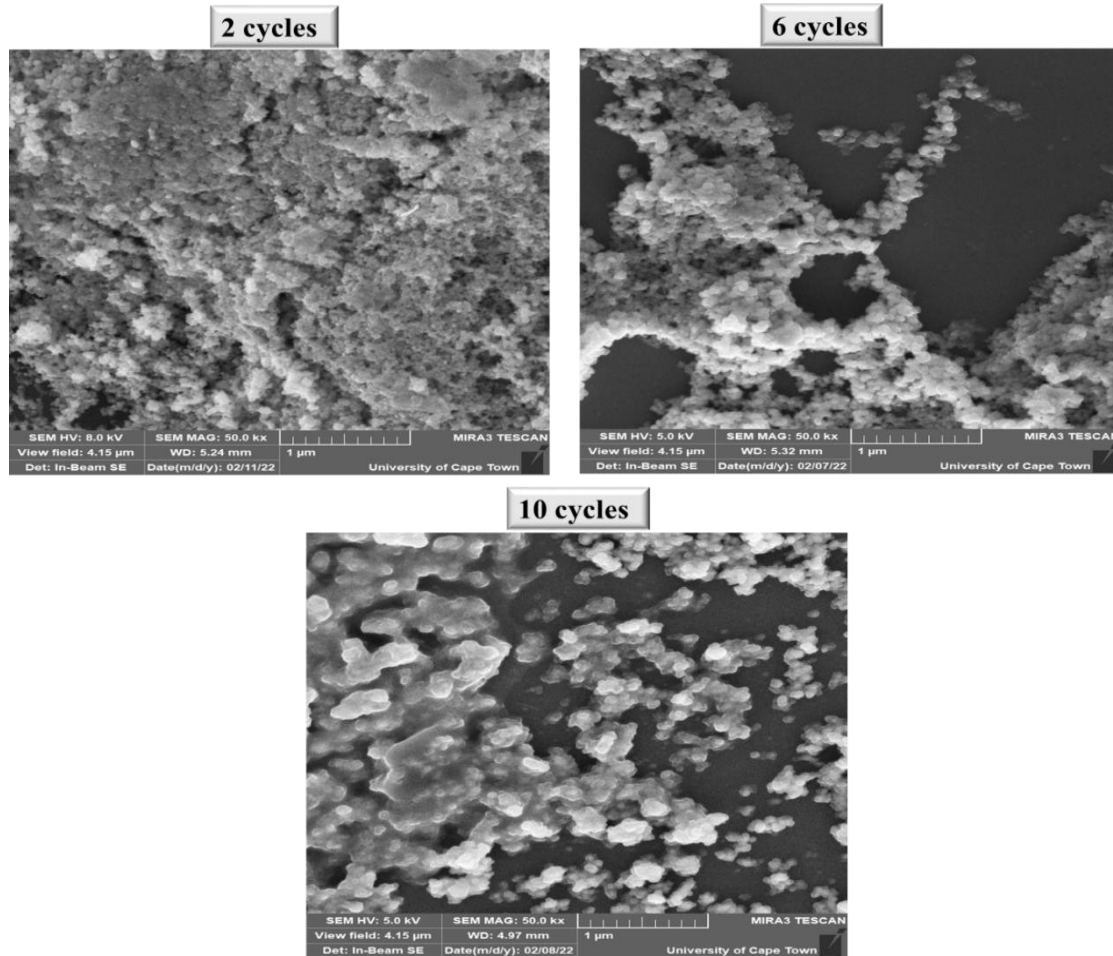


Figure 1: SEM images of the CdSe/CuSesuperlattice thin films deposited at SILAR cycles of 2, 6 and 10

### 3.2    Compositional properties

The EDX spectral patterns obtained from the EDS analysis carried out on the deposited CdSe/CuSe superlattice thin films for the SILAR cycles of 2, 6 and 10 are shown in figure 2. The EDS spectra confirms the presence of copper (Cu), selenium (Se) in addition to elements like carbon (C), oxygen (O), sodium (Na), Magnesium (Mg), silicon (Si) and calcium (Ca). Absence of cadmium in the films could be as a result of weak intercalation of the layers of cadmium selenide and copper selenide thin films. These other elements may be due to the composition of the microscopic glass used for the deposition. The atomic percentages of the elements present in the deposited thin films were presented along with the EDS spectra. It was observed from the figure that increase in SILAR cycle favored the deposition of more layers of copper selenide thin films.

| Elements | C | O | Si | Ca | Cu | Se | Total |
|---|---|---|---|---|---|---|---|
| Atomic (%) | 28.22 | 14.2 | 5.03 | 1.47 | 25.57 | 25.51 | 100 |

| Elements | C | O | Na | Mg | Si | Ca | Cu | Se | Total |
|---|---|---|---|---|---|---|---|---|---|
| Atomic (%) | 11.57 | 16.53 | 3.00 | 1.17 | 7.34 | 2.31 | 31.18 | 26.90 | 100 |

| Elements | C | O | Na | Mg | Si | Ca | Cu | Se | Total |
|---|---|---|---|---|---|---|---|---|---|
| Atomic (%) | 10.68 | 14.52 | 1.59 | 0.47 | 9.25 | 1.71 | 38.88 | 22.89 | 100 |
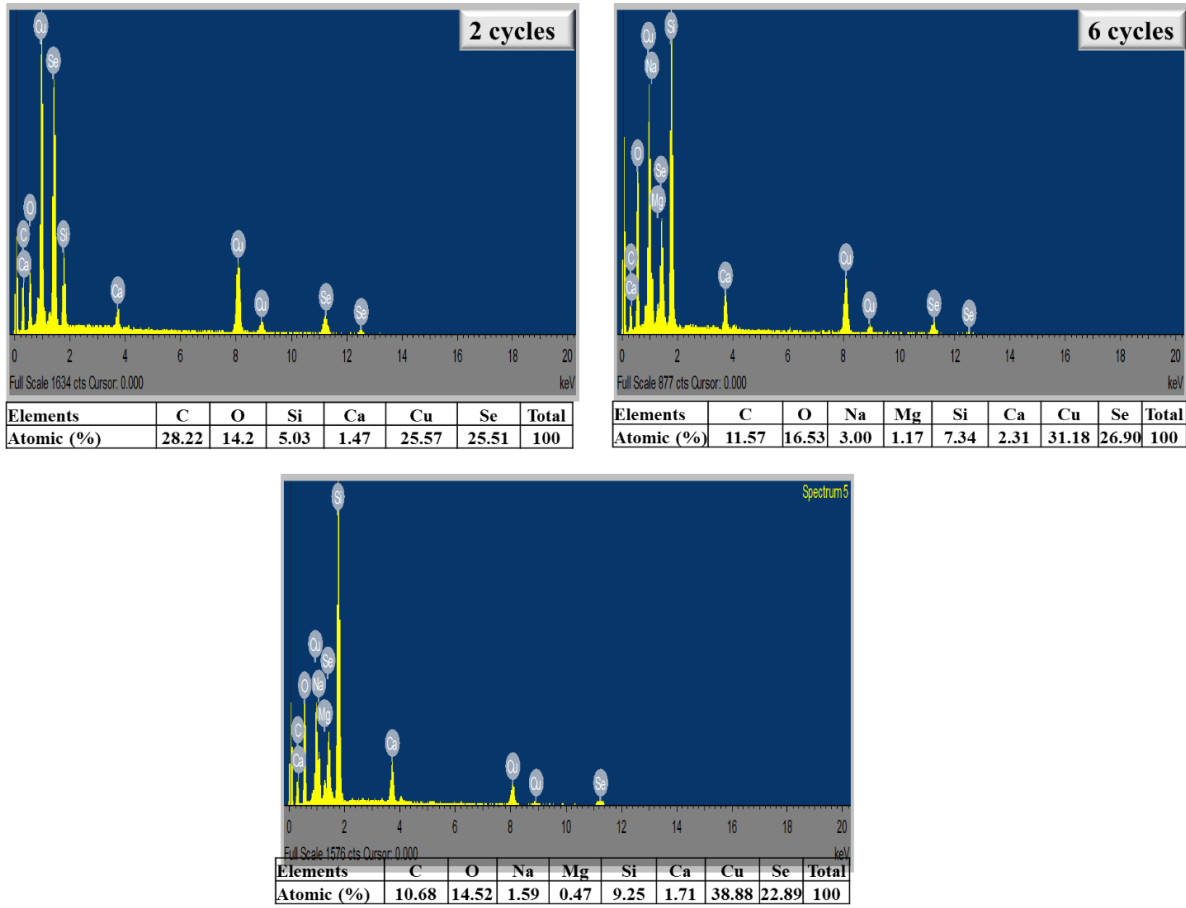
Figure 2: EDS spectra of CdSe/CuSe superlattice thin films deposited under different SILAR cycles of 2, 6 and 10.

### 3.3 Optical properties

Figure 4 is the graph of absorbance against wavelength for the CdSe/CuSe superlattice films deposited at different SILAR cycles measured from vis-spectroscopy machine. The graph showed that the absorbance of the films increased with an increase in the number of SILAR cycles. The absorbance decreases with an increase in wavelength in VIS region but tend to constant values for each of the films in the NIR region. The absorbance of the films of the CdSe/CuSe deposited after 10 cycles has the highest value in the range of 0.75 – 0.45 in the VIS region and 0.45 – 0.50 in the NIR. On the other hand, the film deposited at 2 cycles has lowest value of 0.20 – 0.10 in the VIS and 0.10 in the NIR region.
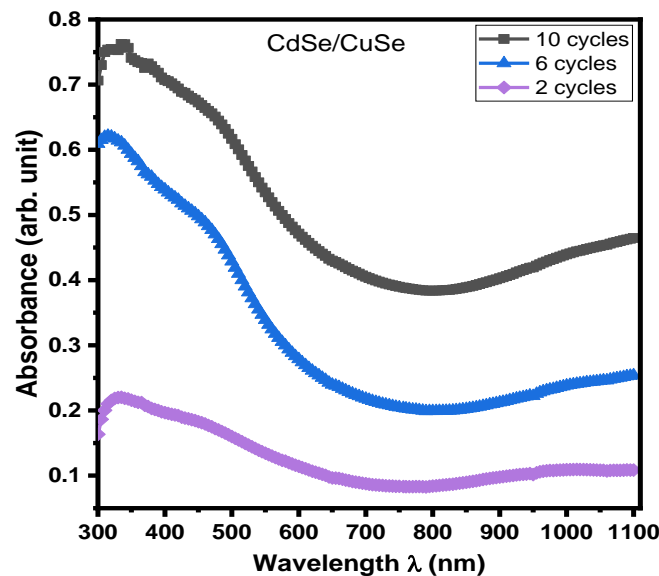
Figure 4: Graph of absorbance against wavelength for CdSe/CuSe thin films

The graph of transmittance against wavelength for deposited superlattice films is dispayed in figure 5. The graph show that the transmittance of the films is high but decreased with an increase in the number of SILAR cycles. The transmittance increases with an increase in wavelength in the VIS region but tends to constant values for each of the films in the NIR region. Maximum transmittance of 77.81% at 1100 nm (NIR region) was observed for film deposited at 2 SILAR cycles while minimum value of 17.28 % at 335 nm (UV region) was observed for film deposited at 10 SILAR cycles. The graph thus showed that the superlattice films have higher transmittance in the NIR region of electromagnetic spectrum and can be used for cold mirror and poultry house coating applications.

The transmittance of the films was evaluated using the relation as given by [44].

$$T = 10^{-A} \qquad\qquad 1$$

Where A is the measured absorbance of the films.
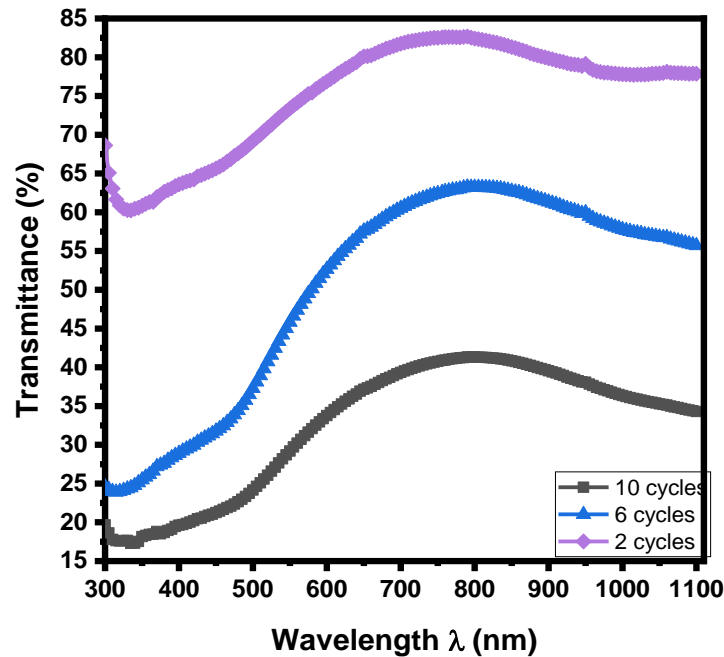
Figure 5: Graph of Transmittance against wavelength for CdSe/CuSe thin films
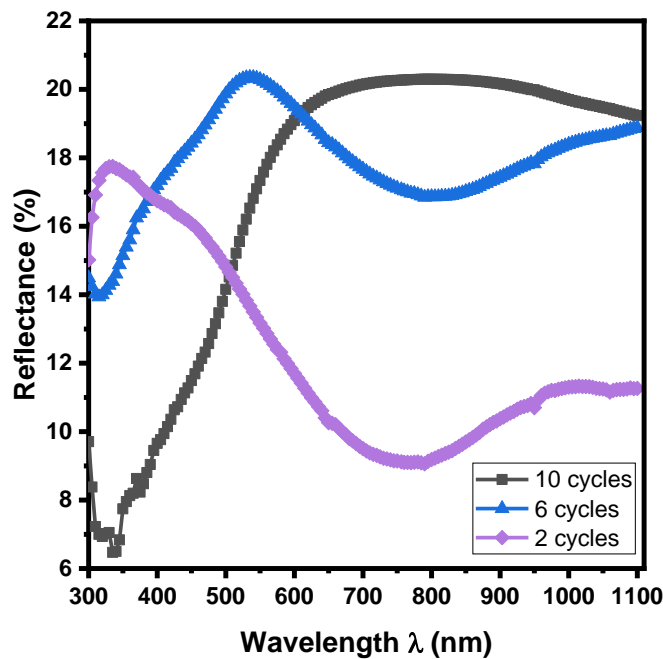
Figure 6: Graph of Reflectance against wavelength for CdSe/CuSe thin films

Figure 6 shows the graph of reflectance against wavelength for the deposited thin films of CdSe/CuSe at different SILAR cycle variations. From the graph, it is observed that the reflectance of the films is ganerally low with maximum reflectance

of 21% exhibited by the film deposited at 8 cycles throughout the VIS and NIR regions. The reflectance increased with an increase in number of SILAR cycles in the NIR region but the maximum reflectance is exhibited by the film 8 cycles in VIS region. The low reflectance exhibited by the films position them for anti-reflection coating applications. The reflectance was calculated using the relation between absorbance (A), transmittance (T) and reflectance (R) as given by [45].

$$R = 1 - (T + A) \hspace{3cm} 2$$
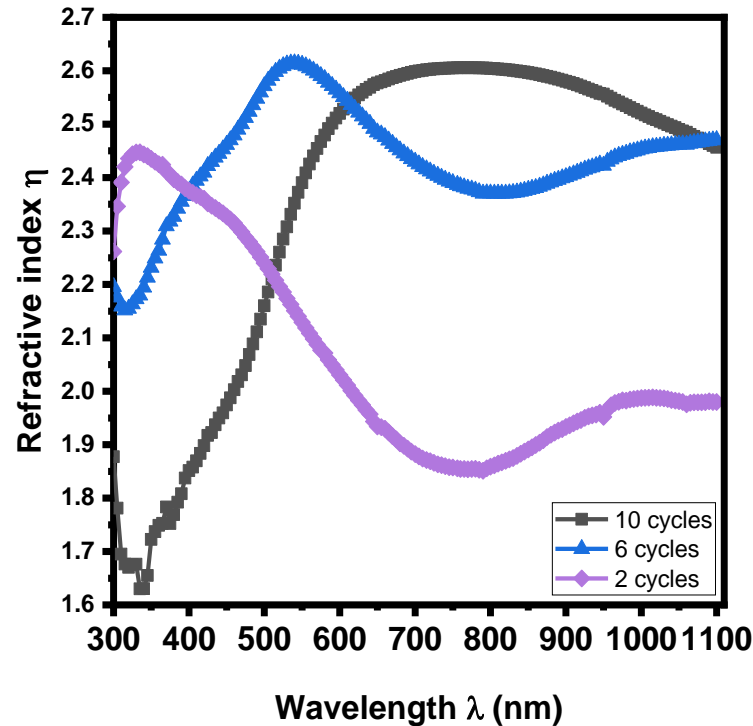


Figure 7: Graph of Refractive index against wavelength for CdSe/CuSe thin films

Figure 7 is the graph of refractive index against wavelength for the deposited thin films at different SILAR cycles. The refractive index was evaluated using the formula given by [46]

$$\eta = \frac{1+R}{1-R} + \sqrt{\frac{4R}{(1-R)^2} - k^2} \hspace{2cm} 3$$

Where k is the extinction coefficient of the films.

The graph showed similar trend to reflectance but the refractive index of the films is generally observed to be high with maximum value of 2.60 exhibited by the films deposited at 8 and 10 cycles in the VIS and NIR regions. The refrative index of the films thus increased with an increase in SILAR cycles in the NIR region while in the VIR region, it initially increased with an increase in SILAR cycles up to 6 and 8 cycles and thereafter decreased to lower values in the range of 1.65 – 2.60 in the region as number of cycles increased to 10 cycles. The range of refractive index of the films in the NIR is 1.85 – 2.60.
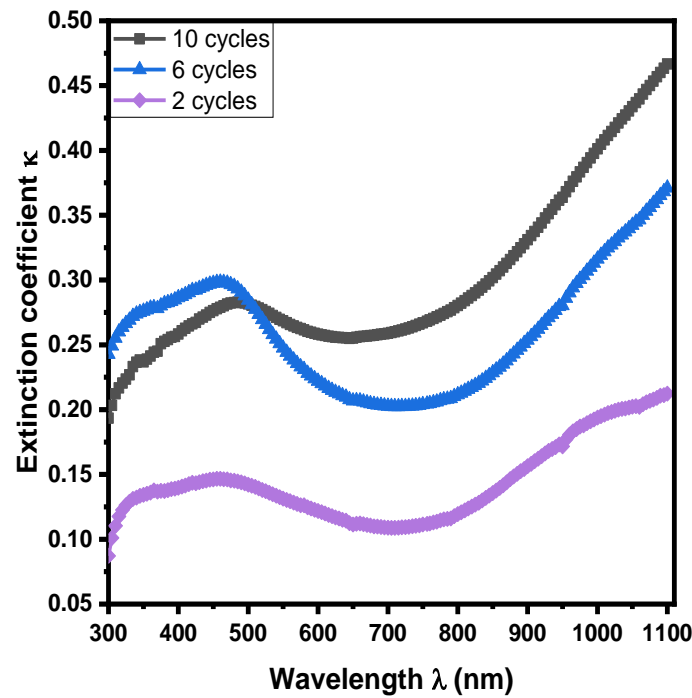
Figure 8: Graph of Extinction coefficient against wavelength for CdSe/CuSe thin films

The plot of extinction coefficient of the superlattice thin films of CdSe/CuSe as a function of wavelength is displayed in figure 8. From the figure, it can be seen that the extinction coefficient of the films is low but increases with an increase in the number of SILAR cycles and wavelength in the NIR region of electromagnetic spectrum. However, the film deposited at 6 cycles has maximum value of 0.30 at wavelength of 450 nm (VIS region) while the films deposited at 2 and 4 cycles have minimum value in the range 0.10 to 0.15 as wavelength increased to 500 nm. The low values of extinction coefficient exhibited by the superlattice films of CdSe/CuSe make them good materials for solar cells and photodetector applications regarding the high transmittance in the NIR region. The extinction coefficient of the films was calculated using the relation given by [47, 48].

$$k = \frac{\alpha\lambda}{4\pi} \qquad 4$$

Where α and λ are the absorption coefficient and wavelength respectively.
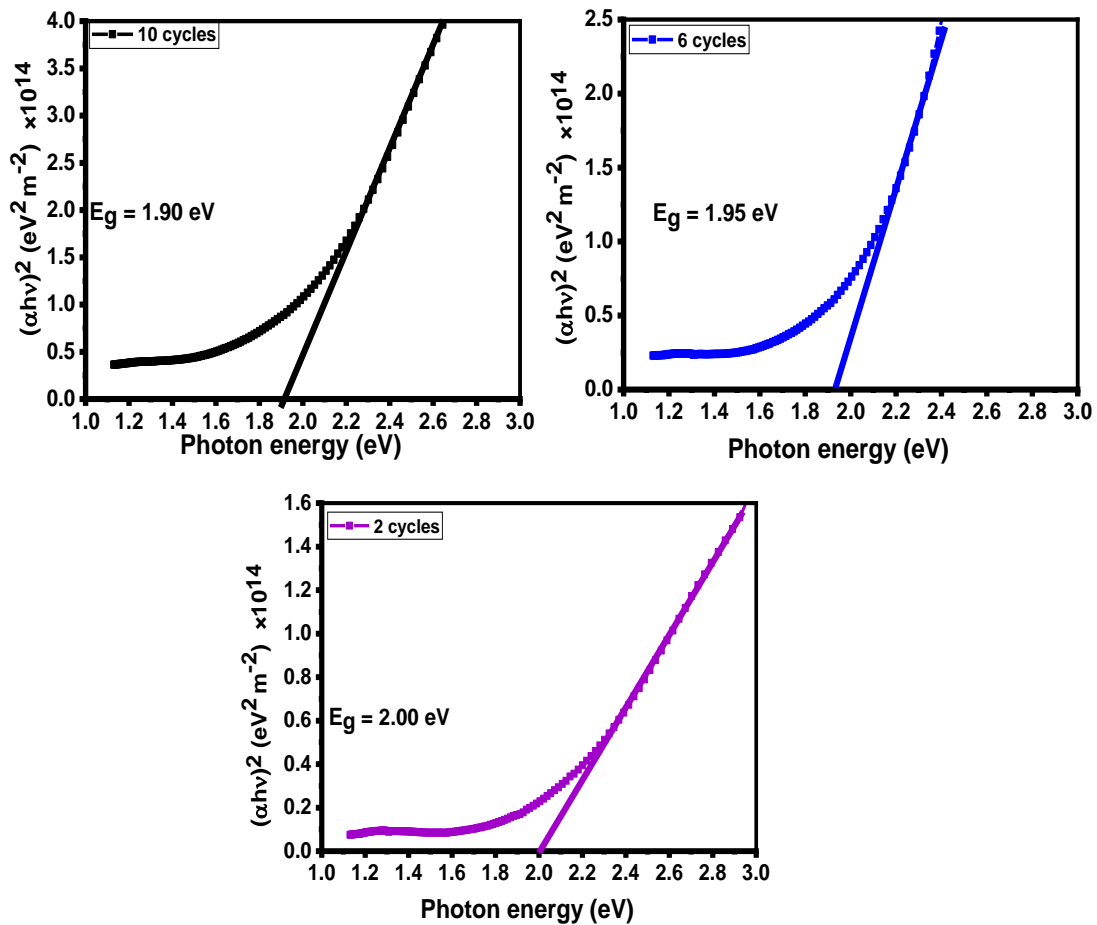
Figure 9: Plots of $(\alpha h\upsilon)^2$ against photon energy for CdSe/CuSe thin films

The plots of $(\alpha h\upsilon)^2$ against photon energy for determination of bandgap energy of the superlattice films of CdSe/CuSe deposited at different SILAR cycle variations is presented in figure 9. Energy bandgap values of the superlattice thin films obtained by extrapolation of the straight part of the graph to the photon energy axis at $(\alpha h\upsilon)^2$ equals to zero were found to be 2.00 eV, 1.95 eV and 1.90 eV for 2, 6 and 10 cycles respectively. These energy bandgap values are in the solar spectrum range and thus could be used in thin film solar cell and many other optoelectronic applications. The bandgap energy was evaluated using the Tauc relation as given by [49].

$$\alpha h\upsilon = B(h\upsilon - E_g)^n \qquad\qquad 5$$

Where $\upsilon$ is the frequency, h is the planck constant, $E_g$ is the bandgap energy, B is a constant and $n$ is the transition form factor (REF).

### 3.4    Film thickness properties

Figure 10 is the plot of film thickness against number SILAR cycles for the deposited CdSe/CuSe thin films. The plot showed that the thickness of the superlattice thin films was found to increase from 112.50 to 152.50 nm as number of SILAR cycles increased from 2 cycles to 10 cycles. This observed increase in film thickness could be ascribed to formation of multilayered nanostructure of cadmium selenide and copper selenide on the surface of the microscopic substrates as number of SILAR cycle increases. Similar trend of increase in film thickness of SILAR deposited thin films as number of SILAR cycles increases has been reported by (50-52).
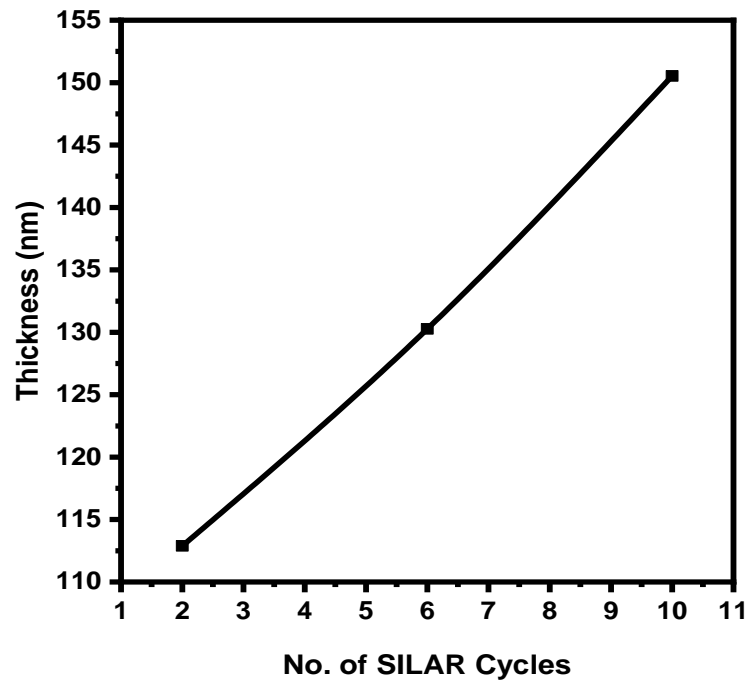
Figure 10: Plot of film thickness against SILAR cycle for the CdSe/CuSe superlattice thin films

### 3.5 Structural properties

Figure 3 shows the x – ray diffraction patterns of as-deposited CdSe/CuSe thin film and CdSe/CuSe thin films deposited at 2, 6 and 10 SILAR cycles of CdSe and CuSe thin films respectively. The x – ray diffractogram of CdSe/CuSe thin film deposited at 2 SILAR cycles showed weak peak that could not be assigned to any phase of either CdSe or CuSe. The observed weak peak could be due to crystallographic defects, strain, or amorphous regions within the interfacial region of the grown superlattice thin film. These can arise due to the early stages of growth and incomplete crystallization during the initial SILAR cycles. Amorphous or poorly crystalline materials can produce broad and weak diffraction peaks that do not correspond to well-defined crystalline phases. Diffractogram of SILAR deposited CdSe/CuSe thin films deposited at 6 and 10 SILAR cycles showed peaks at 28.123 ℃, 31.056 ℃ and 46.102 ℃ with miller indices of (101), (006) and (110) were attributed to hexagonal phase of copper selenide with klockmannite as mineral name. These peaks corresponded to peaks in the standard Powder Diffraction File (PDF) card number 00-034-0171 for hexagonal CuSe. While two peaks observed at 25.533 ℃ and 41.932 ℃ with miller indices of (002)* and (110)* were attributed to hexagonal phase of CdSe with mineral name cadmoselite which corresponded to standard Powder Diffraction File (PDF) card number 00-008-049. The diffraction spectra showed an increase in intensity as number of SILAR cycle increases.
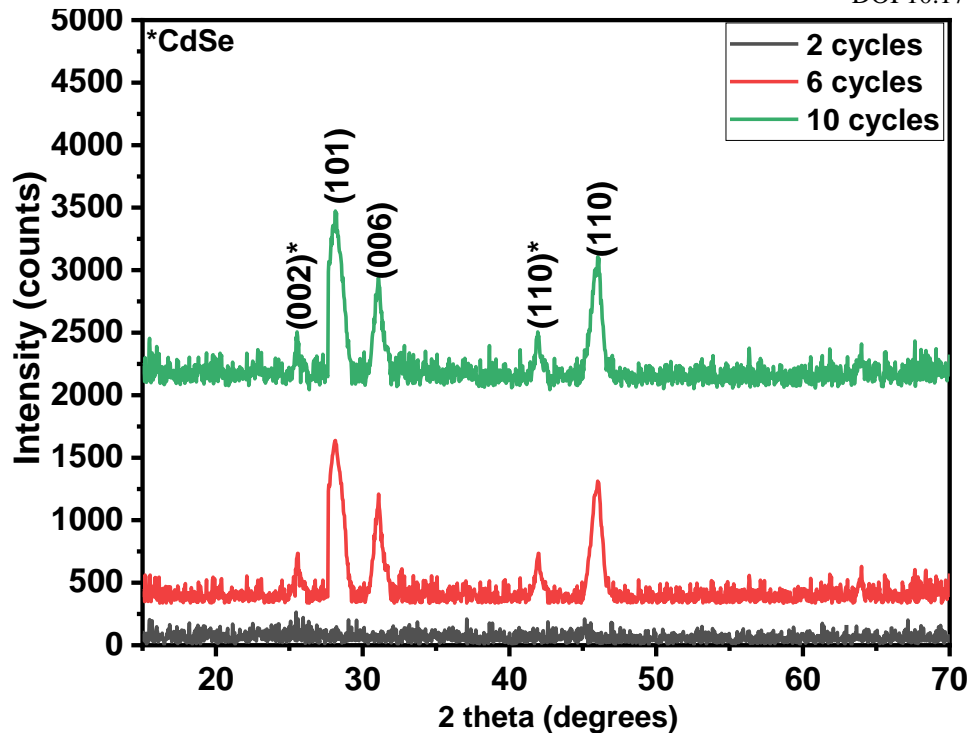
Figure 3: XRD pattern of cadmium selenide/copper selenide (CdSe/CuSe) thin films deposited at 2, 6 and 10 SILAR cycles.

Structural properties such crystallite size, dislocation density and micro-strain were calculated using well known expressions. The crystallite size (D) was calculated using Debye – Scherrer's formula in equation as given by [53].

$$D = \frac{0.9\,\lambda}{\beta\cos\theta} \qquad\qquad 6$$

The dislocation density ($\delta$) of the films was approximated using expression by [54]

$$\delta = \frac{1}{D^2}. \qquad\qquad 7$$

Micro-strain ($\varepsilon$) of the deposited films were approximated using expression as presented by [55]

$$\varepsilon = \frac{\beta}{4\tan\theta} \qquad\qquad 8$$

Where $\beta$ is the full width half maximum (FWHM) of the witnessed $2\theta$ angles, $\theta$ is the diffraction angle, $n$ equals to 1 at minimum dislocation density while $\lambda$ is the wavelength of Cu – k$\alpha$ radiation (1.54059 A) used for the x – ray diffraction experiment. Average crystallite size of the films deposited at 6 and 10 SILAR cycles were found to be 28.59 nm and 31.24 nm. Also, dislocation densities of the films were found to be $5.74 \times 10^{15}$ lines/m$^2$ and $5.18 \times 10^{15}$ lines/m$^2$ while micro-strain values of the films were found to be $8.09 \times 10^{-3}$ and $7.41 \times 10^{-3}$ . This showed that increase in number of SILAR cycles resulted to enhancement in crystallinity of CdSe/CuSe superlattice thin films. These trends highlight that increasing the number of SILAR cycles enhances the overall crystalline quality of the thin films, making them structurally more uniform and stable. This improvement is crucial for applications where the optical and electronic properties of the films are sensitive to their crystallinity and defect levels.

## CONCLUSION

CdSe/CuSe superlattice thin films synthesized using successive ion layer adsorption reaction (SILAR) technique were characterized using SEM, EDX, XRD and UV-VIS spectroscopy analysis to determine their properties for desired applications. The result of SEM analysis showed that CdSe/CuSe superlattice thin films contained agglomerated mass of interconnected spherical-like nanoparticles of different sizes. The EDX characterization showed that the deposited films constitute most of the required elements but copper and selenium been favored most as the number of SILAR cycles increased. The results of the optical analysis showed that the absorbance and extinction coefficient of the films are low but increased with an increase in the number of SILAR cycles. The films generally have low reflectance with the maximum value of 21 % in the VIS/NIR regions while the transmittance is high but decreased with increase in SILAR cycles. The bandgap energy values were found to be 2.00 eV, 1.95 eV and 1.90 eV for films deposited at 2, 6 and 10 cycles. These bandgap values are in the solar spectrum range and could serve as thin film solar cell and many other

International
Multidisciplinary
Research Journal
Reviews (IMRJR)

optoelectronic applications. Structural analysis of the films showed that films grown with high number of SILAR cycles had improved crystal structure. The average crystallite size of the CdSe/CuSe films was found to increase as number of SILAR cycles increased while dislocation density and micro-strain was found to decrease with increase in number of SILAR cycles from 6 to 10.

## REFERENCES

[1]. Almosni, S., Delamarre, A., Jehl, Z., Suchet, D., Cojocaru, L., Giteau, M., Behaghel, B., Julian, A., Ibrahim, C., Tatry, L. & Wang, H. (2018). Material challenges for solar cells in the twenty-first century: directions in emerging technologies. *Science and Technology of Advanced Materials*, 19(1), 336–369. Doi: https://doi.org/10.1080/14686996.2018.1433439

[2]. Hasnain, S. M., Alawaji, S. H., & Elani, U. A. (1998). Solar energy education-a viable pathway for sustainable development. *Renewable Energy*, *14*(1-4), 387-392. Doi: https://doi.org/10.1016/S0960-1481(98)00094-9

[3]. Bourdiros, E. L. (1991). Renewable energy sources education and research as an education for survival. *Progress in solar energy education*, *1*, 12-16.

[4]. Solangi, K. H., Islam, M. R., Saidur, R., Rahim, N. A., & Fayaz, H. (2011). A review on global solar energy policy. *Renewable and sustainable energy reviews*, *15*(4), 2149-2163. Doi: https://doi.org/10.1016/j.rser.2011.01.007

[5]. Hernández-Callejo, L., Gallardo-Saavedra, S., & Alonso-Gómez, V. (2019). A review of photovoltaic systems: Design, operation and maintenance. *Solar Energy*, *188*, 426-440. Doi: https://doi.org/10.1016/j.solener.2019.06.017

[6]. Wang, Q. H., Kalantar-Zadeh, K., Kis, A., Coleman, J. N., & Strano, M. S. (2012). Electronics and optoelectronics of two-dimensional transition metal dichalcogenides. *Nature nanotechnology*, *7*(11), 699-712. Doi: https://doi.org/10.1038/nnano.2012.193

[7]. Gao, M. R., Xu, Y. F., Jiang, J., & Yu, S. H. (2013). Nanostructured metal chalcogenides: synthesis, modification, and applications in energy conversion and storage devices. *Chemical Society Reviews*, *42*(7), 2986-3017. Doi: https://doi.org/10.1039/C2CS35310E

[8]. Petrovic, M., Gilic, M., Cirkovic, J., Romcevic, M., Romcevic, N., Trajic, J. & Yahia, I. (2017). Optical properties of CuSe thin films - band gap determination. *Science of Sintering*, 49, 167-174. Doi: https://doi.org/10.2298/SOS1702167P

[9]. Yadav, A. A. (2014). Nanocrystalline copper selenide thin films by chemical spray pyrolysis. *Journal of Materials Science: Materials in Electronics*, *25*(3), 1251-1257. Doi: https://doi.org/10.1007/s10854-014-1717-5

[10]. Ablekim, T., Duenow, J. N., Zheng, X., Moutinho, H., Moseley, J., Perkins, C. L., Johnston, S. W., O'Keefe, P., Colegrove, E., Albin, D. S., Reese, M. O. & Metzger, W. K. (2020). Thin film solar cells with 19 % efficiency by thermal evaporation of CdSe and CdTe. *ACS Energy Letters,* 5, 892−896. Doi: https://doi.org/10.1021/acsenergylett.9b02836

[11]. El-Menyawy, E. & Azab, A. A. (2018). Optical, electrical and photoelectrical properties of nanocrystalline cadmium selenide films for photosensor applications. *Optik*, 168, 217–227. Doi: https://doi.org/10.1016/j.ijleo.2018.04.056

[12]. Shyju, T. S., Anandhi, S., Indirajith, R., & Gopalakrishnan, R. (2011). Solvothermal synthesis, deposition and characterization of cadmium selenide (CdSe) thin films by thermal evaporation technique. *Journal of Crystal Growth,* 337(1), 38–45. Doi: https://doi.org/10.1016/j.jcrysgro.2011.09.051

[13]. Rosly, H. N., Rahman, K. S., Harif, M. N., Doroody, C., Isah, M., Misran, H. & Amin, N. (2020). Annealing temperature assisted microstructural and optoelectrical properties of CdSe thin film grown by RF magnetron sputtering, *Superlattices and Microstructures*, 148, 106716. Doi: https://doi.org/10.1016/j.spmi.2020.106716

[14]. Rosly, H. N., Rahman, K. S., Abdullah, S. F., Harif, M. N., Doroody, C., Chelvanathan, P., Misran, H., Sopian, K. & Amin, N. (2021). The Role of Deposition Temperature in the Photovoltaic Properties of RF-Sputtered CdSe Thin Films. *Crystals*, 11(73), 1 – 13. Doi: https://doi.org/10.3390/cryst11010073

[15]. Li, C., Wang, F., Chen, Y., Wu, L., Zhang, J., Li, W., He, X., Li, B. & Feng, L. (2018) Characterization of sputtered CdSe thin films as the window layer for CdTe solar cells. *Mater. Sci. Semicond. Process*, 83, 89–95. Doi: https://doi.org/10.1016/j.mssp.2018.04.022

[16]. Mathuri, S., Ramamurthi, K. & Babu, R.R. (2017) Influence of deposition distance and substrate temperature on the CdSe thin films deposited by electron beam evaporation technique. *Thin Solid Film*. 625, 138–147. Doi: https://doi.org/10.1016/j.tsf.2017.01.053

[17]. Sahuban B. M. S., Chandramohan R., Vijayan T. A., Saravana K. S., Sri Kumar S. R., Ayeshamariam, A. & Jayachandran, M. (2016). Effect of Temperature of Electron Beam Evaporated CdSe Thin Films. *Journal of Material Sciences & Engineering,* 5(6), 1 – 5.

[18]. Yang, Q., Zhao, J., Guan, M., Liu, C., Cui, L., Han, D., and Zeng, Y. (2011). Growth and annealing of zinc-blende CdSe thin films on GaAs (001) by molecular beam epitaxy. *Applied Surface Science, 257(21), 9038–9043.* Doi: https://doi.org/10.1016/j.apsusc.2011.05.096

[19]. Elisa, M., Iordache, S.-M., Iordache, A.-M., Rusu, M. I., Socol, G., Filipescu, M., Bartha, C. and Enculescu, M. (2020). Pulsed Laser Deposition Films Based on CdSe-Doped Zinc Aluminophosphate Glass. *The Journal of The Minerals, Metals & Materials Society (TMS)*,73, 495–503. Doi: https://doi.org/10.1007/s11837-020-04150-3

[20]. Shelke, N. T., Karle, S. C., and Karche, B. R. (2020). Photoresponse properties of CdSe thin film photodetector. *Journal of Materials Science: Materials in Electronics,* 31, 15061–15069. Doi: https://doi.org/10.1007/s10854-020-04069-0

[21]. Yadav, A. A., Barote, M. A., and Masumdar, E. U. (2010). Studies on cadmium selenide (CdSe) thin films deposited by spray pyrolysis. *Materials Chemistry and Physics, 121(1-2), 53–57.* Doi: https://doi.org/10.1016/j.matchemphys.2009.12.039

[22]. Hassen, M., Riahi, R., Laatar, F., and Ezzaouia, H. (2020). Optical and surface properties of CdSe thin films prepared by sol-gel spin coating method. *Surfaces and Interfaces*, 18(100408), 1 - 10. Doi: https://doi.org/10.1016/j.surfin.2019.100408

[23]. Hussain S, Iqbal M, Khan AA, Khan MN, Mehboob G, Ajmal S, Ashfaq JM, Mehboob G, Ahmed MS, Khisro SN, Li C-J, Chikwenze R and Ezugwu S (2021). Fabrication of Nanostructured Cadmium Selenide Thin Films for Optoelectronics Applications. *Front. Chem.* 9:661723. Doi: https://doi.org/10.3389/fchem.2021.661723

[24]. Oksuzoglu, F. Gubur, H. M., Havare, A. K., Ozmen, S. I., Unal, M. and Tozlu, C. (2020). Structural properties of cadmium selenide nanowires prepared by chemical bath deposition for the electrical and photosensitive characteristics of the p-Si/CdSe heterojunction. *Journal of Photonics for Energy,* 10(2), 025502. Doi: https://doi.org/10.1117/1.JPE.10.025502

[25]. Kariper, I. A. (2019). A Novel Method for Producing Nanostructured CdSe Thin Film. *Surface Review and Letters,* 27(7), 1950175. Doi: https://doi.org/10.1142/S0218625X19501750

[26]. Piryaei, M., Gholami Hatam, E. & Ghobadi, N. (2017). Influence of pH on the optical, structural and compositional properties of nanocrystalline CdSe thin films prepared by chemical bath deposition. *Journal of Materials Science: Materials in Electronics*, 28,2550–2556. Doi: https://doi.org/10.1007/s10854-016-5830-5

[27]. Gangawane, S. A., Malekar, V. P. & Fulari, V. J. (2020). Surface Deformation of Cadmium Selenide Thin Films By DEHI Technique. *Materials Today: Proceedings,* 23, 276–283. Doi: https://doi.org/10.1016/j.matpr.2020.02.026

[28]. Bai, R., Chaudhary, S. & Pandya, D. K. (2018). Zinc blende to Wurtzite phase shift of CdSe thin films prepared by electrochemical deposition. *AIP Conference Proceedings*, 1942(1), 1 – 4. Doi: https://doi.org/10.1063/1.5029159

[29]. Olusola, O. I., Echendu, O. K. and Dharmadasa, I. (2015). Development of CdSe thin films for application in electronic devices. *Journal of Materials Science: Materials in Electronics*, 26 (2), 1066-1076. Doi: https://doi.org/10.1007/s10854-014-2506-x

[30]. Zafar, H. K., Sohail, M., Nafady, A., Ostrikov, K. K., Will, G., Wahab, M. A., & O'Mullane, A. P. (2023). S-doped copper selenide thin films synthesized by chemical bath deposition for photoelectrochemical water splitting. *Applied Surface Science*, 641, 158505. https://doi.org/10.1016/j.apsusc.2023.158505

[31]. Ghobadi, N., Chobin, S., Rezaee, S., and Shakoury, R. (2020). Tuning the Optical and Photocatalytic Features of Copper Selenide Prepared by Chemical Solution Deposition Method. *Surfaces and Interfaces,* 21(100706), 1 – 7. Doi: https://doi.org/10.1016/j.surfin.2020.100706

[32]. Sadekar, H. K. (2018). Optical and Structural Properties of CuSe Thin Films Deposited by Chemical Bath Deposition (CBD) Technique. *International Research Journal of Science and Engineering,* 2018(A2), 20 – 22. url: https://oaji.net/articles/2017/731-1516001716.pdf

[33]. Thirumavalavan, S., Mani K., & Sagadevan, S (2015). Investigation of the Structural, Optical and Electrical Properties of Copper Selenide Thin Films. *Materials Research, 18*(5), 1000-1007. Doi: https://doi.org/10.1590/1516-1439.039215

[34]. Yadav, B., Singh, P., Yadav, C., Pandey, D. & Singh, D. (2020). Structural and wavelength dependent optical study of thermally evaporated $Cu_2Se$ thin films. *Zeitschrift für Naturforschung A*, 75(9), 781-788. Doi: https://doi.org/10.1515/zna-2020-0098

[35]. Shaikh, A. V., Mane, R. S., Joo, O., Han, S. & Pathan, H. M. (2012). Electrodeposition of Copper Selenide Films from Acidic Bath and their Properties. *AIP Conference Proceedings,*1451, 194 – 196. Doi: https://doi.org/10.1063/1.4732412

[36]. Ramesh, K., Thanikaikarasan, S. & Bharathi, B. (2014). Structural, Morphological and Optical Properties of Copper Selenide Thin Films. *International Journal of ChemTech Research*, 6(13), 5408 – 5411.

[37]. Dhasade, S. S., Thombare, J. V., Gaikwad, R. S., Gaikwad, S. V., Kumbhare, S. S. & Patil, S. (2015). Copper selenide nanorods grown at room temperature by electrodeposition. *Materials Science in Semiconductor Processing*, 30, 48 – 55. Doi: https://doi.org/10.1016/j.mssp.2014.09.021

[38]. Ikhioya, I. L. & Agbakwuru, C. B. (2016). Investigation of the Structural, Electrical and Optical Properties of Copper Selenide Semiconductor Thin Films Deposited by Electrodeposition Techniques. *Journal of the Nigerian Association of Mathematical Physics*, 33, 155 – 160.

[39]. Udofia, K. I. & Okoli, D. N. (2017). Investigation of the Optical, Structural and Surface Morphology Properties of Copper Selenide Thin Films. *International Journal of Scientific Research and Education,* 5(4), 6357 - 6363.

[40]. Hamilton, C. E., Flood, D. J., & Barron, A. R. (2013). Thin film CdSe/CuSe photovoltaic on a flexible single walled carbon nanotube substrate. Physical Chemistry Chemical Physics, 15(11), 3930-3938. Doi: https://doi.org/10.1039/C3CP50435B

[41]. Xu, L., Huang, X., Huang, H., Chen, H., Xu, J., & Chen, K. (1998). Surface modification and enhancement of luminescence due to quantum effects in coated CdSe/CuSe semiconductor nanocrystals. Japanese journal of applied physics, 37(6R), 3491. Doi: https://doi.org/10.1143/JJAP.37.3491

[42]. Kalyanikutty, K. P., Gautam, U. K., & Rao, C. N. R. (2007). Ultra-thin crystalline films of CdSe and CuSe formed at the organic-aqueous interface. Journal of Nanoscience and Nanotechnology, 7(6), 1916-1922. Doi: https://doi.org/10.1166/jnn.2007.741

[43]. Elekalachi, C. I., Ezenwa, I. A., Okereke, A. N., Okoli, N. L & Nwori, A. N. (2023). Influence of Annealing Temperature on the Properties of SILAR Deposited CdSe/ZnSe Superlattice Thin Films for Optoelectronic Applications. J*ournal of Nanoarchitectonics,* 2023, 4(1): 26-44. Doi: https://doi.org/10.37256/nat.4120231650

[44]. Nwori, A. N., Ezenwaka, L. N. Ottih, I. E. Okereke, N. A. & Okoli, N. L (2021). Optical, Electrical, Structural and morphological Properties of Electrodeposited CdMnS Thin Film Semiconductors for Possible Device Applications. Journal of Physics and Chemistry of Materials, 2021, 8(2): 1-11. Doi: https://doi.org/10.21467/jmm.8.1.40-51

[45]. Nwori, A. N., Okoli, N. L, Okereke, N. A, Ottih, I. E & Ezenwaka, L. N. (2022). Optical Properties of Electrodeposited CdMnS Thin Film Semiconductor Alloys for Optoelectronics Applications: Effect of Deposition Potential. *Journal of Nano and Material Science Research*, 1, 58-67. url: https://journals.nanotechunn.com/jnmsr/article/view/7

[46]. Nwori, A. N., Ezenwaka, L. N., Ottih, I. E., Okereke, N. A & Okoli, N. L (2022). Study of the Optical, Structural and Morphological Properties of Electrodeposited Copper Manganese Sulfide (CuMnS) Thin Films for Possible Device Applications. *Trends in Sciences,* 19(17): 1-11. Doi: https://doi.org/10.48048/tis.2022.5747

[47]. Ezenwaka L. N., Okoli, N. L., Okereke, N. A., Ezenwa, I. A. & Nwori, A. N. (2022) Properties of electrosynthesized cobalt doped zinc selenide thin films deposited at varying time. *Journal of Nanoarchitectonics,* 3(1): 1-17. Doi: https://doi.org/10.37256/nat.3120221040

[48]. Ezenwaka, L. N., Nwori, A. N, Ottih, I. E. Okereke, N. A. & Okoli, N. L. (2022). Investigation of the Optical, Structural and Compositional Properties of Electrodeposited Lead Manganese Sulfide (PbMnS) Thin Films for Possible Device Applications. J*ournal of Nanoarchitectonics,* 3(1): 18-32. Doi: https://doi.org/10.37256/nat.3120221226

[49]. Nwori, A. N., Ezenwaka, L. N., Ottih, I. E., Okereke, N. A. & Okoli, N. L (2021). Study of the Optical, Electrical, Structural and Morphological Properties of Electrodeposited Lead Manganese Sulphide (PbMnS) Thin Film Semiconductors for Possible Device Applications. *Journal Modern Materials*, 8(1): 40-51. Doi: https://doi.org/10.21467/jmm.8.1.40-51

[50]. Nkamuo, C. J., Okoli, N. L. & Igweze, D. C. (2021). Results of SILAR Cycles Variation on the Optical, Structural and Electrical Properties of Lead Iodide Thin Films. *Applied Physics*, 4(3), 31-39. Doi: https://doi.org/10.31058/j.ap.2021.43003

[51]. Santhamoorthy, A., Srinivasan, P., Krishnakumar, A., Rayappan, J. B. B., & Babu, K. J. (2021). SILAR-deposited nanostructured ZnO thin films: effect of deposition cycles on surface properties. Bulletin of Materials Science, 44(3), 1-8. Doi: https://doi.org/10.1007/s12034-021-02465-8

[52]. Egwunyenga, N. J., Onuabuchi, V. C., Okoli N. L. & Nwankwo I. E. (2021). Effect of SILAR Cycles on the Thickness, Structural, Optical Properties of Cobalt Selenide Thin Films, International Research Journal of Multidisciplinary Technovation, 3(4), 1–9. Doi: https://doi.org/10.34256/irjmt2141

[53]. Ikhioya, I. mosobomeh L., Akpu, N. I., Onoh, E. U., Aisida, S. O., Ahmad, I., Maaza, M., & Ezema, F. I. (2023). Enhanced physical properties of nickel telluride metal chalcogenide material with molybdenum dopant. Materials Research Innovations, 28(1), 40–48. Doi: https://doi.org/10.1080/14328917.2023.2222465

[54]. Salahi, E., Enayati Taloobaghi, H., Shahidi, M. M., & Ezema, F. I. (2024). Investigating the Dielectric Photosensitivity of Zinc Oxide Nanostructures Under Ultraviolet Light. Nano-Horizons: Journal of Nanosciences and Nanotechnologies, 3, 12. Doi: https://doi.org/10.25159/3005-2602/14260

[55]. Asogwa, L.I., Nkele, A.C., Ezekoye, V.A., Awada, C. Alshoaibi, A., Nwanya, A. C., Nwulu, N. & Ezema, F. I. (2024). Synthesis, characterization, and comparative study of titanium dioxide and methyl ammonium lead iodide perovskite doped with cesium. Indian J Phys. 1-11. Doi: https://doi.org/10.1007/s12648-024-03290-5